Determination of the Conformational Flexibility of Methyl α-Cellobioside in Solution by NMR Spectroscopy and Molecular Simulations

E. Andreas Larsson, Mikael Staaf, Peter Söderman, Christer Höög, and Göran Widmalm*

Department of Organic Chemistry, Arrhenius Laboratory, Stockholm University, S-106 91 Stockholm, Sweden

Received: January 20, 2004; In Final Form: March 2, 2004

The conformational flexibility of methyl α-cellobioside in water and dimethyl sulfoxide solutions was investigated by 1D ^{1}H,^{1}H T-ROESY experiments. In combination with molecular dynamics simulations, effective proton−proton distances could be derived using experimentally determined cross-relaxation rates. An anti-ψ-conformational state was present in both solvents confirming a previous flexibility hypothesis at this torsion angle. In water solution, an anti-ϕ-conformational state was also detected and quantified. These results show that already at the disaccharide level a large flexibility is present at the glycosidic linkage. In addition to the syn-conformation which is present to ∼93% for the title compound in water solution, the minor anti-ϕ- and anti-ψ-conformational states are populated to ∼2% and ∼5%, respectively.

Introduction

Carbohydrates play many important roles in Nature ranging from construction materials to energy storage. In biological systems, they are involved in recognition processes in the form of glycoconjugates, most often as glycolipids and glycoproteins. From a structural point of view, the study of cellulose, which is a homopolymer made of β-(1→4)-linked glucosyl residues, is of paramount importance due to its ubiquitous presence and the huge number of products made thereof.[1] It is furthermore of fundamental interest to understand the conformational and dynamical behavior at the glycosidic linkage connecting the sugar residues into higher oligomers and subsequently into polymers.

Due to its vast occurrence and its availability, studies on the conformation of cellobiose and derivatives thereof have been performed for many decades.[2−14] It is now well accepted that a syn-conformation, in which the protons at the glycosidic linkage are on the same side compared to a plane perpendicular to the corresponding C−H bonds, is the global conformation in solution. However, more recently, indications of an anti-conformation at the ψ torsion angle have been proposed to be present to a considerable (detectable) degree.[15] The presence of such a conformation is certainly of importance since the accessible conformational space thereby increases significantly and will have great impact on how oligo- and polysaccharide dynamics should be interpreted.

To address these questions, we have chosen methyl α-cellobioside **1** (Figure 1) as a model, since NMR spectral overlap is reduced compared to the β-anomeric form.[16] The conformational flexibility is investigated in both dimethyl sulfoxide (DMSO) and water solutions with the aid of ^{1}H,^{1}H T-ROESY experiments and molecular dynamics simulations with explicit water as solvent. We also utilize a selectively deuterated analogue **1-*d*** of methyl α-cellobioside, since selective elimination of the H4 spin from the relaxation pathway was not possible.[17] This study extends our previous investigation on **1** which addressed preferences of folded vs extended conformations.[18] In addition, we investigate the possible presence of an anti-ϕ-conformation at the glycosidic linkage. To the best of our knowledge, this is the first time the presence and quantification of the three conformational states responsible for the major degrees of flexibility are described at the disaccharide level for a compound such as cellobiose. Previously, a similar conformational flexibility has been documented for a *C*-glycoside analogue of lactose in which the glycosidic oxygen was exchanged for a methylene group.[19]

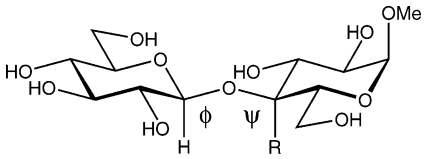

1 R = H
1-*d* R = ^{2}H

Figure 1. Schematic of the disaccharide β-D-Glc*p*-(1→4)-α-D-Glc*p*-OMe (**1**) and its deuterated analogue **1-*d***.

Results and Discussion

Water is the natural solvent for carbohydrates. However, solvent mixtures and polar aprotic solvents such as DMSO facilitate further insight into molecular structure and solvation including a preference for certain functional groups or regions.[20−22] The investigation of conformational preferences in **1** thus employs water and DMSO as solvents.

Some time ago Dabrowski and co-workers reported that deuterium isotope effects were possible to observe for the hydroxyl groups in the ^{1}H NMR spectrum of partially deuterium exchanged β-D-Gal*p*-(1→3)-β-D-Glc*p*-OMe (**2**) in DMSO solution.[23,24] This finding was reproducible in our laboratory. Their results were interpreted as the existence of an anti-conformer at the ψ-torsion angle of the glycosidic linkage between the two sugar residues, schematically depicted in Figure 2a. However, we were not able to detect such an effect for **1** (Figure 2b), which would have indicated the presence of an anti-ψ-conformation, previously discussed based on our computational and experimental NMR work.[18] Therefore, we chose an approach based on the nuclear Overhauser effect.

* Corresponding author. Email: gw@organ.su.se.

10.1021/jp049714c CCC: $27.50
Published on Web 04/10/2004

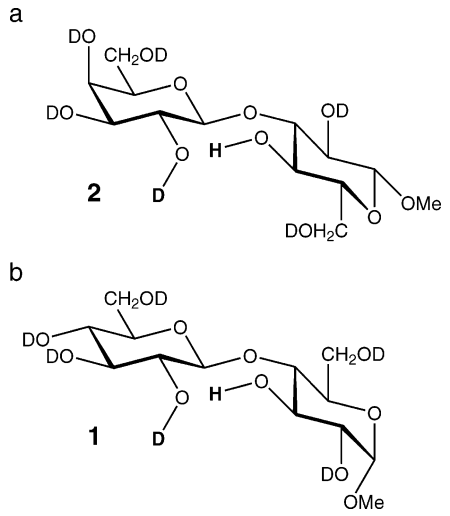

Figure 2. Schematic of β-D-Gal*p*-(1→3)-β-D-Glc*p*-OMe (**2**) and β-D-Glc*p*-(1→4)-α-D-Glc*p*-OMe (**1**) in their respective anti-ψ-conformation. For each disaccharide, one of the two possible *H*/*D* isotopomers that may give rise to isotope effects observable in the ^{1}H NMR spectrum of the disaccharides in DMSO-d_6 is depicted in bold.

Proton−proton relaxation for molecules in solution is dominated by the dipole−dipole cross-relaxation between spins that are close in space. The strength of these interactions is dependent on the molecular dynamics, the internuclear distance(s), and the number of interacting spins. The ^{1}H,^{1}H NOE is sensitive to $\omega\tau_c$, where ω is the spectrometer frequency in radians and τ_c is the correlation time of the molecule.[25] Certain combinations lead to a zero-crossing when it is not possible to detect the NOE, which occurs when $\omega\tau_c = \sqrt{5/4}$. At a ^{1}H Larmor frequency of 600 MHz, conditions close to the above prevail in both solvents for **1**, making accurate measurements of cross-relaxation rates difficult. Under these conditions, the use of rotating-frame Overhauser effect spectroscopy will alleviate these problems.[26] However, experimental problems with signals arising from TOCSY transfer may be significant. A modified multiple-pulse spin-lock has therefore been proposed, which efficiently suppresses such signals.[27,28] The multiple-pulse or transverse ROE (T-ROE) cross-relaxation rate, σ_{T-ROE}, can be calculated as the mean of σ_{NOE} and σ_{ROE} as described by eq 1:

$$\sigma_{T-ROE} = \frac{1}{8}(D_{HH})^2[6J(2\omega) + 3J(\omega) + J(0)] \qquad (1)$$

The dipolar coupling constant, $D_{HH} = (\mu_0/4\pi)\gamma^2\hbar r^{-3}$, is a measure of the strength of the dipolar interaction, where μ_0 is the permeability in a vacuum, γ is the magnetogyric ratio for protons, $\hbar$ is Planck's constant divided by 2π, and r is the distance between interacting protons.

In one of our earlier studies, we described that certain relaxation pathways can be neglected when a ^{1}H spin is substituted by ^{2}H.[29] Furthermore, when spectral resolution prevents the elimination of a spin in a multiple relaxation pathway, the use of chemical synthesis remains the only viable way of solving the problem.

^{1}H,^{1}H T-ROE buildup curves were obtained by selective excitation of resonances from anomeric protons in **1** (Figure 3). The ^{1}H,^{1}H cross-relaxation rates, σ, were obtained as the initial slopes and are compiled in Table 1. Due to spectral overlap, not all correlations observed in DMSO could be quantified in water solution. In **1** the key T-ROE was the transglycosidic one between H1′ and H4 (Figure 4a), whereas in

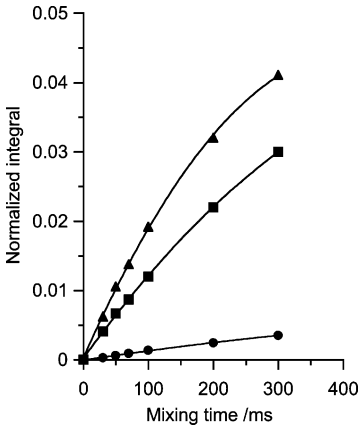

Figure 3. Experimental ^{1}H,^{1}H T-ROE buildup curves of **1** in DMSO-d_6 solution for the inter-residue H1′−H4 pair (▲), the intraresidue H1−H2 spin-pair (■), and the inter-residue H1′−H3 pair (●).

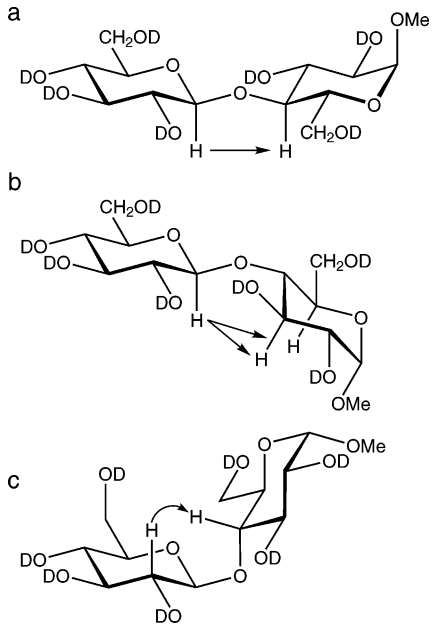

Figure 4. Schematic of **1** in (a) syn-conformation showing spatial proximity between H1′ and H4, (b) anti-ψ-conformation depicting the proximity between H1′ and H3/H5, and (c) anti-ϕ-conformation in which H2′ and H4 are close in space.

TABLE 1: Experimental Cross-Relaxation Rates, σ_{T-ROE} (s^{-1}), at 303 K for Methyl α-Cellobioside (1) and Methyl α-(4-^{2}H)-cellobioside (1-*d*) in DMSO-d_6 and in D_2O, Calculated by Second-Order Polynominal Fits of Normalized Integrals

proton pair		DMSO-d_6		D_2O	
excited	detected	**1**	**1-*d***	**1**	**1-*d***
H1′	H3	0.016	0.015		0.009
H1′	H4	0.195		0.139	
H1′	H5	0.016	0.009		
H1	H2	0.112	0.123	0.098	0.097

1-*d* focus was put on H1′ to H3 and H5 (Figure 4b). One may note that the two latter T-ROEs are possible to quantify in DMSO, but that the H1′−H3 is consistent between the two samples, whereas the H1′−H5 T-ROE shows a σ that is different between the two samples.

Unknown distances, r_{ij}, between protons i and j can be obtained by the isolated spin-pair approximation (ISPA)[30,31] by comparing the cross-relaxation rate of the reference spin pair, σ_{ref} to that of i and j, σ_{ij}, according to eq 2:

$$r_{ij} = r_{ref}(\sigma_{ref}/\sigma_{ij})^{1/6} \quad (2)$$

The reference distance, r_{ref}, is to be chosen for protons residing in a well-defined part of the molecule. The H1−H2 distance obtained from molecular modeling (vide infra) was used as the reference distance, and the resulting proton−proton distances are shown in Table 2. In DMSO, the trans-glycosidic H1′−H4 distance in **1** is short, ∼2.2 Å. The H1′−H3 pair shows a similar distance of ∼3.4 Å in both **1** and **1-*d***, whereas this is not the case for H1′−H5. In water solution, the derived distances are slightly longer. The difference between the two solvents indicates a small conformational change or altered sampling within the conformational wells. The reason may be attributed to the presence of an internal hydrogen bond between O5′ and HO3 in DMSO solution, whereas in water the hydrogen bond is not present to any significant amount.[32] These results will be used in the analysis of the conformational flexibility of **1** presented below.

Proton−proton distances can also be calculated from cross-relaxation rates using the "model-free" approach,[33] provided that the motional parameters are known. The molecular motions are then described by correlation times for a slow global motion, τ_M, and a local motion, τ_e. Prerequisites are that the different motions are uncorrelated and that the molecule reorients isotropically. The restriction of the internal motion is described by a generalized order parameter, S^2, which adopts values between 0 and 1, with $S^2 = 1$ corresponding to a fully restricted internal motion. If τ_e is much shorter than τ_M and S^2 is close to unity, the model-free spectral density, $J(\omega)$, has the following form [eq 3]:

$$J(\omega) = \frac{2}{5}\left(\frac{S^2\tau_M}{1 + \omega^2\tau_M{}^2}\right) \quad (3)$$

Our previous ^{13}C relaxation study of disaccharides in DMSO solution,[34] which was used to obtain conditions out of the extreme narrowing regime, gave motional parameters for **1**, viz., $\tau_M = 0.32$ ns and $S^2 \approx 0.85$. Employing eqs 1 and 3 as previously described,[35] we obtain proton−proton distances in **1** (Table 2). Notably, the proton−proton distances derived using the dynamics obtained from the ^{13}C relaxation measurements show excellent agreement with those calculated via the ISPA approach. Thus, additional credence to the description of the dynamics with a correlation time for rotational reorientation, τ_M, together with rapid internal dynamics of limited amplitude as described by the generalized order parameter S^2.

The conformation at a glycosidic linkage may be described by a single energy minimum around which sampling occurs in a dynamic manner, the interconversion between two regions, often along the ψ torsion angle, or the population of several conformational states. An initial estimate of glycosidic torsion angles and proton−proton distances was obtained from a Monte Carlo (MC) simulation employing the Hard Sphere *Exo*-Anomeric (HSEA) approach.[36] The simulations sampled the syn- and the anti-ψ-conformational wells, respectively, and the results are compiled in Table 3. As anticipated, the syn-conformation shows a short H1′−H4 distance of ∼2.4 Å and long H1′−H3 and H1′−H5 distances > 4 Å. For the anti-ψ-conformation the reverse behavior is observed with slightly altered distances. Due to the difference for the H1′−H5 distance between **1** and **1-*d***, this distance was judged less reliable for the comparison and consequently the H1′−H3 distance, which also could be obtained in water solution, was chosen in a two-state analysis.

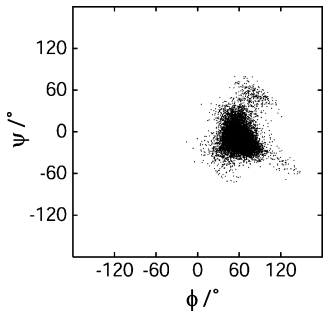

Figure 5. Scatter plot of ϕ vs ψ in **1** from MD simulation I.

TABLE 2: Experimental Inter-Proton Distances *r* (Å) for Methyl α-Cellobioside, Using the Model-Free Approach and ISPA

proton pair	DMSO-d_6				D_2O	
	model-free[a]		ISPA[b]		ISPA	
	1	**1-*d***	**1**	**1-*d***	**1**	**1-*d***
H1′−H3	3.38	3.42	3.36	3.45		3.58
H1′−H4	2.23		2.21		2.29	
H1′−H5	3.38	3.72	3.36	3.76		
H1−H2	2.45	2.40	2.40[c]	2.40	2.40	2.40

[a] Calculated using eqs 1 and 3 with $\tau_M = 0.32$ ns and $S^2 = 0.85$. [b] Calculated using eq 2. [c] Reference distance from MD simulation.

TABLE 3: Glycosidic Torsion and Bond Angles (deg) and Inter-Proton Distances *r* (Å) from Simulations of 1 Averaged According to $1/r = \langle r^{-6}\rangle^{1/6}$

conformation	simulation	$\langle\phi\rangle$	$\langle\psi\rangle$	$\langle\tau\rangle$	$r_{H1'-H3}$	$r_{H1'-H4}$	$r_{H1'-H5}$
syn	MC	52	2	117.0[a]	4.49	2.38	4.07
	MD	61	−9	116.6	4.45	2.39	4.05
anti-ψ	MC	37	−179	119.9[a]	1.96	3.65	2.38
	MD	52	−168	119.9	2.26	3.58	2.77
anti-ϕ	MD	166	4	118.3	4.45	3.53	4.39

[a] Fixed angle.

The experimental data together with proton−proton distances from simulations may be used in a two state analysis:

$$(1 - x)\langle r_{syn}{}^{-6}\rangle + (x)\langle r_{anti}{}^{-6}\rangle = r_{exp}{}^{-6} \quad (4)$$

where x is the fraction that populates the anti-conformation. Rearrangement of eq 4 leads to

$$x = \frac{r_{exp}{}^{-6} - \langle r_{syn}{}^{-6}\rangle}{\langle r_{anti}{}^{-6}\rangle - \langle r_{syn}{}^{-6}\rangle} \quad (5)$$

from which the degree of the anti-ψ-conformation can be calculated. Combining the results from the MC simulations with those from NMR experiment leads to $x = 0.03$ for **1** in DMSO and $x = 0.02$ in water solution. Thus, a small amount of anti-ψ-conformation is indeed present.

Employing a full molecular mechanics force field, in contrast to the simplified approach used in the initial analysis, in the form of a molecular dynamics (MD) simulation with explicit water molecules should give an improved description of the conformational preferences for **1**. The MD simulation starting from the syn-conformation did not show any transitions out of the global energy minimum well during 3 ns (Figure 5), and the conformational flexibility within this well should be satisfactorily described. Therefore, another simulation was started form the anti-ψ-conformational state (Figure 6). After ∼0.6 ns of the production run, a transition out of this well took place, resulting in a syn-conformation. However, the sampling

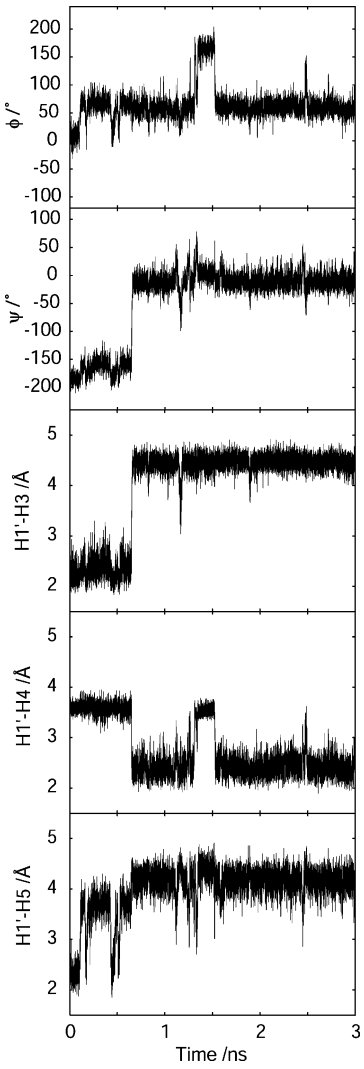

Figure 6. Time dependence of torsion angles and selected proton−proton distances in **1** from MD simulation II.

of the degrees of freedom within the well should still be sufficient for an adequate description of the conformational freedom within the well. Most interestingly, the H1′−H3 distance is short, H1′−H4 distance is long, but H1′−H5 distance depends on the ϕ/ψ-conformational pair fluctuations. Thus, the latter is not a good choice in the comparison. In addition, the anti-ϕ-conformational state was populated for a brief period, ∼1.3−1.5 ns, which facilitated the calculation of motionally averaged distances also within this well. The analysis shows that determination of the degree of anti-ψ is not sensitive to the amount of anti-ϕ (cf. Table 3).

Hydrogen bonding was analyzed in the syn state (simulation I) which showed the presence of HO6′ to O3 for 57% of the simulation time, and in addition also HO3 to O5′ with a 9% prevalence. For the anti-ψ-conformational state, in simulation II, the importance of direct hydrogen bonding between the two sugar residues was low, since the HO3 to O2′ and HO2′ to O3 hydrogen bonds were present only 12% and 5%, respectively, within this conformational well.

The degree of anti-ψ-conformation analyzed as above shows $x = 0.070$ in DMSO and $x = 0.047$ in water; i.e., slightly larger populations are concluded from analysis with a more complex force field in which additional degrees of freedom are allowed to relax and where the energy wells are more shallow than in the simplified force field. Recent calculations of the potential of mean force in water for β-cellobiose reveal that in addition to the global energy minimum with a syn-conformation, in which the H1′ and H4 protons are on the same side compared to a plane perpendicular to the corresponding C−H bond vectors, both the anti-ϕ- and anti-ψ-conformational states are present to some extent of similar populations, with a small predominance for the former.[37] We therefore investigated the presence of an anti-ϕ-conformational state by selective excitation of the H2′ resonance followed by cross-relaxation to H4 (Figure 4c) and H4′, where the latter is used as a reference distance, $r_{H2',H4'} = 2.70$ Å. In the syn-conformation, the trans-glycosidic distance $r_{H2',H4} = 4.41$ Å, whereas, in the anti-ϕ-conformation, $r_{H2',H4} = 2.22$ Å. It may be noted that also in the anti-ψ-conformation the distance is long with $r_{H2',H4} = 4.71$ Å. The relative ratio of the cross-relaxation rates $\sigma_{H2',H4'}/\sigma_{H2',H4} = 9.1$, which using eq 2 for the syn/anti-ϕ pair gave an experimentally determined distance of $r_{H2',H4} = 3.90$ Å. Subsequent application of eq 5 results in an anti-ϕ population $x = 0.018$. Thus, also for this torsion angle, an anti-conformation is present, although to a smaller extent than predicted for β-cellobiose. When taken together, we obtain for the three conformational states the following relative populations in water solution: 0.93 for syn, 0.05 for anti-ψ, and 0.02 for anti-ϕ.

These above results are quite reasonable, since for disaccharides the anti-ψ-conformational state has been shown to exist in **2** and the anti-ϕ-conformational state is populated ∼5% in β-D-Gal*p*-(1→3)-β-D-Gal*p*NAc-OMe.[38] Anti-conformations are also present in trisaccharides[39,40] and larger oligosaccharides,[41] but then their presence may be due to in some respect spatial interactions changing the shape and the relative energy difference between the populated wells on the potential energy surface. The conformational transitions to the anti-conformers should take place on a slow time scale, on the order of several nanoseconds or even significantly longer, compared to the correlation time of the global reorientation motion of the disaccharide that usually is on the sub-nanosecond time scale. The implications for polymer dynamics in general and cellulose in particular pose interesting problems to be addressed in future studies of complex oligo- or polysaccharides.

Materials and Methods

General. The syntheses of the disaccharides β-D-Glc*p*-(1→4)-α-D-Glc*p*-OMe (**1**) and β-D-Glc*p*-(1→4)-α-D-(^{2}H)-Glc*p*-OMe (**1-*d***) have been described previously.[16,42] The synthesis of β-D-Gal*p*-(1→3)-β-D-Glc*p*-OMe (**2**) employed an AgOTf-promoted glycosylation of methyl 2-*O*-benzyl-4,6-*O*-benzylidene-β-D-glucopyranoside (1 equiv) with 2,3,4,6-tetra-*O*-acetyl-α-D-galactopyranosyl bromide (3 equiv) in the presence of collidine (0.9 equiv) at −30 °C to yield the protected analogue in 87% yield. The disaccharide was deprotected via treatment by sodium in liquid ammonia,[43] consecutive re-*O*-acetylation with acetic anhydride in pyridine, and finally *O*-deacetylation with sodium methoxide in methanol. Purification using gel permeation chromatography gave the target disaccharide, having NMR spectral data in complete agreement with those previously published.[44] Atoms in the terminal residue are denoted by a prime, and in the *O*-methyl residue, the atoms are unprimed. The torsion angles at the glycosidic linkage between the sugar residues are denoted by ϕ = H1′−C1′−O4−C4 and ψ = C1′−O4−C4−H4.

NMR Spectroscopy. Spectra were obtained in 5 mm NMR tubes using a Varian Inova 600 spectrometer operating at 600 MHz, equipped with a triple resonance pulsed field gradient probe. NMR samples for *H*/*D* isotope effect measurements were lyophilized from H_2O or a 2:1 mixture of H_2O:D_2O and prepared

as 10 mM solutions in DMSO-d_6 and recorded at 20 °C. NMR samples: for the 1D T-ROE experiments, samples were prepared as 100 mM solutions of the disaccharides in D_2O or DMSO-d_6. The solutions were treated with CHELEX 100 in order to remove any paramagnetic ions present, and the NMR tubes were sealed under vacuum after three freeze−pump−thaw cycles.

Proton−proton cross-relaxation rates (σ_{T-ROE}) were measured at 30 °C using the one-dimensional DPFGSE T-ROESY experiment.[45−47] Selective excitations at the resonances for anomeric protons were enabled using i-Snob-2 shaped pulses[48] of 17, 24, or 34 ms duration. The gradient durations in the initial DPFGSE part were 1 ms, and the strengths were 0.1 and 0.9 G cm^{-1}. The T-ROESY spin-lock was applied with $\gamma B_1/2\pi = 2.5$ kHz. Spectra were recorded using a spectral width of 3000 Hz and 16k complex points, sampling 304−896 transients at each mixing time. The total relaxation delay between transients was 12 s, i.e., always $>5\ T_1$. Eight different cross-relaxation delays (mixing times) of 0.03, 0.05, 0.07, 0.10, 0.20, 0.30, 0.50, and 0.80 s were used. Prior to Fourier transformation, the FIDs were zero-filled once and multiplied with a 1 Hz exponential line-broadening factor. Spectra were baseline corrected using a first-order correction and integrated using the same integration limits at all mixing times.

Integrated auto-peaks were fitted to an exponential decaying function, and normalized cross-relaxation integrals were obtained by division of the measured integrals from the extrapolated auto-peak values at zero mixing time. The regression coefficients in the fits were $R > 0.999$ for the auto-peaks. Cross-relaxation buildup curves were obtained from the normalized integrals at different mixing times, and the rates were calculated by fitting a second-order polynomial using mixing times not longer than 300 ms. The least-squares fits, expressed using the regression coefficient, were found to be $R > 0.998$ in all cases. In D_2O solution, the H3 and H5 resonances overlap severely. Therefore, the H3 signal being a doublet in **1-*d*** was quantified from its downfield resonance, which was possible to integrate separately and subsequently doubled to yield the appropriate integral.

In addition to the above-described procedures, the 1D DPFGSE T-ROESY experiment was performed with selective excitation of the H2′ resonance via i-Snob-2 shaped pulses of 45 ms duration corresponding to a width of 38 Hz. The mixing times used in this case were 0.20 and 0.30 s. Integration of the H4 and H4′ resonances were used to calculate the relative cross-relaxation rates from H2′.

Computer Simulations. Metropolis Monte Carlo simulations[49] were carried out using the GEGOP program[50] (version 2.7) with a force field based on the HSEA approach which makes use of rigid pyranoid sugars. The simple potential includes only the ϕ-torsion and van der Waals interactions. A total of 10^6 Monte Carlo steps was performed for each simulation starting from either a syn- or an anti-ψ-conformation. The resulting acceptance ratios were 41% in the former and 34% in the latter simulation. The glycosidic torsion angles were not allowed to move more than 20° in an MC step. The MC simulations were performed on an O_2 workstation (SGI, CA).

The molecular mechanics program CHARMM[51] (parallel version, C25b2) was used for the molecular dynamics (MD) simulations with the force field PARM22 (Molecular Simulations Inc., San Diego, CA), which is similar to the carbohydrate force field developed by Ha et al.[52] Initial conditions for simulation of **1** were prepared by placing the disaccharide in a previously equilibrated cubic water box of length 29.972 Å containing 900 TIP3P water[53] molecules and removing those waters that were closer than 2.5 Å to any solute atom. This procedure resulted in a system with the disaccharide and 855 waters which was energy minimized using Steepest Descent, 200 steps, followed by Adopted Basis Newton−Raphson until the root-mean-square gradient was less than 0.01 kcal mol^{-1} Å^{-1}. Velocities were initialized at 100 K followed by heating at 5 K increments during 8 ps to 300 K, where the systems were equilibrated for 200 ps. Constant temperature simulations were then performed using Berendsen's weak-coupling algorithm.[54] Periodic boundary conditions and the minimum image convention were used together with a heuristic nonbond frequency update, a force shift cutoff acting to 12 Å, and a dielectric constant of unity. SHAKE, with a tolerance gradient of 10^{-4}, was used to restrain hydrogen-heavy atom bond stretch;[55] the time step was accordingly set to 2 fs. Data were saved every 0.2 ps for analysis. The geometric criteria for hydrogen bonding was set to an oxygen−hydrogen distance < 2.5 Å and a donor-hydrogen···acceptor angle $\Theta > 135°$. MD simulations were performed on an IBM SP2 computer at the Center for Parallel Computers, KTH, Stockholm, using 16 nodes resulting in a CPU time of approximately 20 h per 1 ns.

Acknowledgment. This work was supported by a grant from the Swedish Research Council. We thank the Center for Parallel Computers, KTH, Stockholm, for putting computer facilities at our disposal.

References and Notes

(1) Klemm, D.; Philipp, B.; Heinze, T.; Heinze, U.; Wagenknecht, W. *Comprehensive cellulose chemistry, Vol. 1: Fundamentals and analytical methods*; Wiley-VCH: Weinheim, 1998.
(2) Bentley, R. *J. Am. Chem. Soc.* **1959**, *81*, 1952−1956.
(3) Melberg, S.; Rasmussen, H. *Carbohydr. Res.* **1979**, *71*, 25−34.
(4) Lipkind, G. M.; Verovsky, V. E.; Kochetkov, N. K. *Carbohydr. Res.* **1984**, *133*, 1−13.
(5) Kroon-Batenburg, L. M. J.; Kroon, J.; Leeflang, B. R.; Vliegenthart, J. F. G. *Carbohydr. Res.* **1993**, *245*, 21−42.
(6) Hardy, B. J.; Sarko, A. *J. Comput. Chem.* **1993**, *14*, 831−847.
(7) Hardy, B. J.; Sarko, A. *J. Comput. Chem.* **1993**, *14*, 848−857.
(8) Kroon-Batenburg, L. M. J.; Kruiskamp, P. H.; Vliegenthart, J. F. G.; Kroon, J. *J. Phys. Chem. B* **1997**, *101*, 8454−6459.
(9) Bernet, B.; Vasella, A. *Helv. Chim. Acta* **2000**, *83*, 2055−2071.
(10) Bernet, B.; Xu, J.; Vasella, A. *Helv. Chim. Acta* **2000**, *83*, 2072−2114.
(11) Sugiyama, H.; Hisamichi, K.; Usui, T.; Sakai, K.; Ishiyama, J.-i. *J. Mol. Struct.* **2000**, *556*, 173−177.
(12) Mendonca, S.; Johnson, G. P.; French, A. D.; Laine, R. A. *J. Phys. Chem. A* **2002**, *106*, 4115−4124.
(13) Strati, G. L.; Willett, J. L.; Momany, F. A. *Carbohydr. Res.* **2002**, *337*, 1833−1849.
(14) Strati, G. L.; Willett, J. L.; Momany, F. A. *Carbohydr. Res.* **2002**, *337*, 1851−1859.
(15) Lipkind, G. M.; Shashkov, A. S.; Kochetkov, N. K. *Carbohydr. Res.* **1985**, *141*, 191−197.
(16) Backman, I.; Erbing, B.; Jansson, P.-E.; Kenne, L. *J. Chem. Soc., Perkin Trans. 1* **1988**, 889−898.
(17) Dixon, A. M.; Widmalm, G.; Bull, T. E. *J. Magn. Reson.* **2000**, *147*, 266−272.
(18) Hardy, B. J.; Gutierrez, A.; Lesiak, K.; Seidl, E.; Widmalm, G. *J. Phys. Chem.* **1996**, *100*, 9187−9192.
(19) Asensio, J. L.; Espinosa, J. F.; Dietrich, H.; Cañada, F. J.; Schmidt, R. R.; Martín-Lomas, M.; André, S.; Gabius, H.-J.; Jiménez-Barbero, J. *J. Am. Chem. Soc.* **1999**, *121*, 8995−9000.
(20) Bagno, A. *J. Phys. Org. Chem.* **2002**, *15*, 790−795.
(21) Angulo, M.; Hawat, C.; Hofmann, H.-J.; Berger, S. *Org. Biomol. Chem.* **2003**, *1*, 1049−1052.
(22) Siebert, H.-C.; André, S.; Vliegenthart, J. F. G.; Gabius, H.-J.; Minch, M. J. *J. Biomol. NMR* **2003**, *25*, 197−215.
(23) Dabrowski, J.; Kožár, T.; Grosskurth, H.; Nifant'ev, N. E. *J. Am. Chem. Soc.* **1995**, *117*, 5534−5539.
(24) Dabrowski, J.; Grosskurth, H.; Baust, C.; Nifant'ev, N. E. *J. Biomol. NMR* **1998**, *12*, 161−172.
(25) Neuhaus, D.; Williamson, M. *The Nuclear Overhauser Effect in Structural and Conformational Analysis*; VCH Publishers: New York, 1989.

(26) Bothner-By, A. A.; Stephens, R. L.; Lee, J.-m.; Warren, C. D.; Jeanloz, R. W. *J. Am. Chem. Soc.* **1984**, *106*, 811−813.
(27) Hwang, T.-L.; Shaka, A. J. *J. Am. Chem. Soc.* **1992**, *114*, 3157−3159.
(28) Hwang, T.-L.; Shaka, A. J. *J. Magn. Reson. B* **1993**, *102*, 155−165.
(29) Widmalm, G.; Byrd, R. A.; Egan, W. *Carbohydr. Res.* **1992**, *229*, 195−211.
(30) Keepers, J. W.; James, T. L. *J. Magn. Reson.* **1984**, *57*, 404−426.
(31) Thomas, P. D.; Basus, V. J.; James, T. L. *Proc. Natl. Acad. Sci. U.S.A.* **1991**, *88*, 1237−1241.
(32) Leeflang, B. R.; Vliegenthart, J. F. G.; Kroon-Batenburg, L. M. J.; van Eijck, B. P.; Kroon, J. *Carbohydr. Res.* **1992**, *230*, 41−61.
(33) Lipari, G.; Szabo, A. *J. Am. Chem. Soc.* **1982**, *104*, 4546−4559.
(34) Söderman, P.; Widmalm, G. *Magn. Reson. Chem.* **1999**, *37*, 586−590.
(35) Mäler, L.; Widmalm, G.; Kowalewski, J. *J. Phys. Chem.* **1996**, *100*, 17103−17110.
(36) Thøgersen, H.; Lemieux, R. U.; Bock, K.; Meyer, B. *Can. J. Chem.* **1982**, *60*, 44−57.
(37) Kuttel, M. M. *Simulations of Carbohydrate Conformational Dynamics and Thermodynamics*, Ph.D. Thesis, University of Cape Town, 2003.
(38) Bukowski, R.; Morris, L. M.; Woods, R. J.; Weimar, T. *Eur. J. Org. Chem.* **2001**, 2697−2705.
(39) Landersjö, C.; Stenutz, R.; Widmalm, G. *J. Am. Chem. Soc.* **1997**, *119*, 8695−8698.
(40) Dixon, A. M.; Venable, R.; Widmalm, G.; Bull, T. E.; Pastor, R. W. *Biopolymers* **2003**, *69*, 448−460.
(41) Masoud, H.; Perry, M. B.; Brisson, J.-R.; Uhrin, D.; Richards, J. C. *Can. J. Chem.* **1994**, *72*, 1466−1477.
(42) Söderman, P.; Widmalm, G. *J. Org. Chem.* **1999**, *64*, 4199−4200.
(43) Philips, K. D.; Žemlička, J.; Horwitz, J. P. *Carbohydr. Res.* **1973**, *30*, 281−286.
(44) Nifant'ev, N. E.; Amochaevan, V. Y.; Shashkov, A. S.; Kochetkov, N. K. *Carbohydr. Res.* **1993**, *250*, 211−230.
(45) Stott, K.; Stonehouse, J.; Keeler, J.; Hwang, T.-L.; Shaka, A. J. *J. Am. Chem. Soc.* **1995**, *117*, 4199−4200.
(46) Stott, K.; Keeler, J.; Van, Q. N.; Shaka, A. J. *J. Magn. Reson.* **1997**, *125*, 302−324.
(47) Kjellberg, A.; Widmalm, G. *Biopolymers* **1999**, *50*, 391−399.
(48) Kupče, E.; Boyd, J.; Campbell, I. D. *J. Magn. Reson. B* **1995**, *106*, 300−303.
(49) Peters, T.; Meyer, B.; Stuike-Prill, R.; Somorjai, R.; Brisson, J.-R. *Carbohydr. Res.* **1993**, *238*, 49−73.
(50) Stuike-Prill, R.; Meyer, B. *Eur. J. Biochem.* **1990**, *194*, 903−919.
(51) Brooks, B. R.; Bruccoleri, R. E.; Olafson, B. D.; States, D. J.; Swaminathan, S.; Karplus, M. *J. Comput. Chem.* **1983**, *4*, 187−217.
(52) Ha, S. N.; Giammona, A.; Field, M.; Brady, J. W. *Carbohydr. Res.* **1988**, *180*, 207−221.
(53) Jorgensen, W. L.; Chandrasekhar, J.; Madura, J. D.; Impey, R. W.; Klein, M. L. J. *J. Chem. Phys.* **1983**, *79*, 926−935.
(54) Berendsen, H. J. C.; Postma, J. P. M.; van Gunsteren, W. F.; DiNola, A.; Haak, J. R. *J. Chem. Phys.* **1984**, *81*, 3684−3690.
(55) van Gunsteren, W. F.; Berendsen, H. J. C. *Mol. Phys.* **1977**, *34*, 1311−1327.